



Published in final edited form as:

Microcirculation. 2010 July ; 17(5): 333–347. doi:10.1111/j.1549-8719.2010.00034.x.

Collateral Capillary Arterialization following arteriolar ligation in murine skeletal muscle

Feilim Mac Gabhann and Shayn M. Peirce

Department of Biomedical Engineering, University of Virginia, Charlottesville, VA

Abstract

OBJECTIVE—Chronic and acute ischemic diseases – peripheral artery disease, coronary artery disease, stroke – result in tissue damage unless blood flow is maintained or restored in a timely manner. Mice of different strains recover from arteriolar ligation (by increasing collateral blood flow) at different speeds. We quantify the spatio-temporal patterns of microvascular network remodeling following arteriolar ligation in different mouse strains to better understand interindividual variability.

METHODS—Whole-muscle spinotrapezius microvascular networks of mouse strains C57Bl/6, Balb/c and CD1 were imaged using confocal microscopy following ligation of feeding arterioles.

RESULTS—Baseline arteriolar structures of C57Bl/6 and Balb/c mice feature heavily ramified arcades and unconnected dendritic trees, respectively. This network angioarchitecture identifies ischemia-protected and ischemia-vulnerable tissues: unlike C57Bl/6, downstream capillary perfusion in Balb/c spinotrapezius is lost following ligation. Perfusion recovery requires arterialization (expansion and investment of mural cells) of a subset of capillaries forming a new low-resistance collateral pathway between arteriolar trees. Outbred CD1 exhibit either Balb/c-like or C57Bl/6-like spinotrapezius angioarchitecture, predictive of response to arteriolar ligation.

CONCLUSIONS—This collateral capillary arterialization process may explain the reported longer time required for blood flow recovery in Balb/c hindlimb ischemia, as low-resistance blood flow pathways along capillary conduits must be formed (‘arterialization’) before reperfusion.

INTRODUCTION

Ischemic diseases include peripheral artery disease, coronary artery disease, and ischemic stroke, caused by occlusion of upstream arteries feeding skeletal muscle, heart muscle or brain. There has been much focus on the evaluation of risk factors for the occurrence of ischemic events in humans, however there is also inter-individual variation in the severity of the injury following the event. In this study we use mouse strains as a surrogate for interindividual variability, demonstrating that the *microvascular phenotype* of an individual strongly determines the severity of injury and the ensuing microvascular response.

Several differences in the outcomes of ischemic injury have been observed between mouse strains. Compared to the more ischemia-protected strains such as C57Bl/6 or 129, Balb/c mice experience the following: severe tissue necrosis following hindlimb ischemia, up to and including limb loss [3,6,9]; larger brain infarct size following non-reversed ligation of

Correspondence: Feilim Mac Gabhann, CSEB 316A, 3400 N. Charles St., Johns Hopkins University, Baltimore MD 21218, feilim@jhu.edu.

DISCLOSURES

None.

the middle cerebral artery [1,10,14]; and higher susceptibility to myocarditis-induced cardiac injury [8]. This consistency between pathological consequences in different tissues suggests that individuals may be placed on a continuum from ischemia-vulnerable to ischemia-protected, applicable to all the tissues. In this case, we are referring to the vulnerability to damaging effects of ischemic injury; this is distinct from the risk of an ischemic injury occurring, which may also be different between strains, but not necessarily in the same direction.

The ischemic insult – in mouse models or in human disease – is typically at the macrovascular level, ligation or internal blockage of the large-diameter femoral, cerebral or coronary arteries. However, the pathological tissue damage that can result from ischemia is a local event, due to a loss of blood flow to local microvascular (arteriole and capillary) networks. Similarly, the restoration of blood flow to an ischemic volume is typically a result of changes at the microvascular level, e.g. arteriogenesis, the expansion of preexisting arteriolar collateral vessels to carry and reroute more blood and compensate for loss elsewhere [13]. Therefore, we investigated the morphology of the microvascular networks and their microvascular remodeling response following arteriolar ligation in different mouse strains.

Here we present the first whole-network and capillary-level view of the microvascular networks of whole mouse skeletal muscles. Morphological microvascular differences between mouse strains have been noted previously; in particular, the density of arteriole-to-arteriole connections (a measure of the ability of a tissue to efficiently re-route flow around a blockage) is significantly lower in the jejunum and pial circulations[3], and thus our first goal was to quantify the characteristic arteriolar connectivity in skeletal muscle of multiple mouse strains. Building on this, we were able to simultaneously visualize both the perfusion of the tissue and the microvascular remodeling responses at five time points following ligation of an upstream arteriole in multiple strains of mouse. By comparing the functional and structural changes that follow vascular occlusion across several mouse backgrounds, dynamically over several days, we gained insight into the responses of ischemia-vulnerable and ischemia-protected mice, and the basis for their relative vulnerability or protection. Along with the reproducible similarity of inbred mouse strain vascular networks, we also tested outbred mice to quantify the vulnerability to loss of perfusion of vascular networks in the skeletal muscle of these more varied mouse backgrounds. It should be noted that in this study we did not assay whether ligation-reduced blood flow failed to match metabolic demands of the tissue, however our observations of complete flow loss, followed by microvascular responses, suggest that arteriolar ligation is a significant stimulus and that ischemia is likely present as it is in femoral artery ligation.

The primary muscle we used for these studies was the mouse spinotrapezius arteriolar ligation model [2]. The spinotrapezius is an accessible tissue: the surgery is quick, minimally invasive (a small dorsal skin incision, no penetration of major body cavities), and well-tolerated. In addition, the muscle is thin and flat, allowing us to image the whole muscle microvasculature *en face* using confocal microscopy. We also used two other flat (though thicker) muscles for comparison, the latissimus dorsi and the thoracic diaphragm.

In our previous study of spinotrapezius artery ligation in C57Bl/6 mice, we observed an increase in arteriolar density, both by intravital and immunofluorescent measurements [2]. In addition, the ligation resulted in significant increases in the tortuosity of the muscle arterioles. Here, we extended the ligation model to other inbred mouse strains, and we used fluorescent perfusion labeling to test whether the ligations resulted in transient or chronic downstream ischemia, assayed by loss of perfusion specifically. We hypothesized that C57Bl/6 mice experience arteriolar remodeling because it is these vessels that experience

changes in blood flow. This suggests that for Balb/c mice, with few arteriole-diameter collaterals, any remodeling should take place at the capillary level, and our study shows for the first time remodeling of capillaries into arterioles following loss of perfusion or ischemia.

Based on these studies of inbred mouse strains, we further hypothesized that outbred mice, which exhibit intrastrain variability in their microvascular architecture, would respond to arteriolar ligation based on their microvascular structural phenotype. That is, we predicted that outbred mice with arteriolar network structure characteristics similar to Balb/c mice would exhibit a Balb/c-like microvascular remodeling response. Thus, phenotype (network architecture) is a high information content readout of the genotype, and can be used as a predictor of ischemic severity and microvascular response. In testing this hypothesis with an outbred strain of mouse, we have now shown for the first time that the baseline microvascular morphology of the spinotrapezius determines both the loss of perfusion indicative of ischemia and the structural microvascular remodeling response to the changes in blood flow.

Finally, we developed a theoretical model of a tissue fed by multiple arterioles that predicts the protective impact of small numbers of arteriole-to-arteriole collaterals against vulnerability to ischemia. This gives us, for the first time, a metric that quantifies the benefit of having an ischemia-protected, highly-connected arteriolar network. In addition, it gives us quantitative insight into the level of connectivity that would be required to significantly reduce this vulnerability in individuals that are at risk for ischemic events. In other words, we can use this model as a tool to compare the difficulty of inducing additional arteriole-to-arteriole collaterals with the benefit obtained. This ability to predict the benefit of even moderate vascular remodeling changes, along with our mouse model of ischemia vulnerability to test interventions, can greatly aid development of preemptive therapies.

METHODS

Mice and study overview

All surgical protocols were approved by the Animal Care and Use Committee of the University of Virginia. Male and female mice (age 8–12 weeks) of the following strains were included in this study: C57Bl/6 (Harlan); Balb/c (Harlan); CD1 (Harlan and from colonies); A/J (Harlan). Mice heterozygous for VEGFR1 (CD1 background) were a kind gift of Guo-Hua Fong (University of Connecticut) and Vicki Bautch (University of North Carolina) and were bred in-house. To establish baseline skeletal muscle microvascular structure, the two spinotrapezius muscles of at least 6 mice per strain were extracted following euthanasia, stained with immunofluorescent markers for vascular structures (arterioles, capillaries and venules), whole-mounted and imaged using a confocal microscope. To determine the impact of mouse strain on vascular response to ischemia, some mice underwent surgical ligation of a supplying arteriole 0, 1, 2, 4 or 7 days prior to tissue harvest. The ligation procedure as outlined in [2] was modified slightly to include two ligations and an incision, similar to femoral ligations [3], and is described in detail in the Supplementary Methods.

Perfusion labeling

To visualize loss of perfusion in the spinotrapezius, perfused capillaries were identified by intravascular delivery of fluorescently-labeled lectin (IB4-Alexa488, Sigma) into anesthetized mice. The jugular vein of the mouse was surgically exposed and 250 μ L of lectin-PBS solution (concentration: 0.1 mg/ml; 25 μ g total lectin) slowly injected using a 27-gauge insulin syringe. Pressure was briefly manually applied to the vein following needle

withdrawal to prevent blood loss. Topical adenosine solution (70 mg/L) was applied to the spinotrapezius to dilate vessels. The mouse was euthanized 10 minutes later by i.p. injection of pentobarbital (0.25 mg/kg), perfusion-fixed using 4% paraformaldehyde, and the tissues harvested and stained as described below.

Harvest and Staining of wholemount tissues

The twin spinotrapezius muscles (both left and right) from euthanized, fixed (4%-paraformaldehyde-perfused) mice were stripped of fascia, undermined, excised and stored in cold PBS prior to staining. In solution, the muscles were washed, permeabilized, and stained for smooth muscle α -actin (SM α A, arteriole/venule stain, IA4-Cy3, Sigma 1 mg/ml); and lectin (capillary stain, IB4-Alexa647, Invitrogen 1 mg/ml) at room temperature for one hour and overnight at 4°C. For lectin-perfused tissues, a different color lectin was used as a 'superfusion' comparison of all capillaries versus perfused capillaries. The tissues were washed and mounted on slides for whole-tissue and confocal imaging.

Image processing and feature quantification

The collection, pseudocoloring and quantification (using ImageJ [11]) of images is described in detail in Supplementary Methods.

Statistics

One-way ANOVA, two-way ANOVA and Student's t-test were used to compare measurements and test for significance, as appropriate and noted in figure legends. P-values for statistical significance are given in each figure legend.

Calculation of ischemia probabilities

To quantify the effect of arteriole-to-arteriole connections on the vulnerability of a tissue to ischemic injury, we used Monte Carlo simulations of tissue arteriolar structure. We started with tissues fed by between 2 and 8 nonintersecting arterioles. To each of these tissues we added a number of arteriole-to-arteriole connections (0–50); each of these connections was stochastically generated by randomly and non-uniquely choosing two of the feeding arterioles. Connecting an arteriole to itself represented a loop within that structure and was permitted. Multiple connections between the same two input arterioles were also permitted. The linking of two previously nonintersecting arterioles resulted in the protection of these vessels should an occlusion occur in one of them.

For each number of input arterioles, we ran the simulation 10,000 times, with different randomly generated arteriole-to-arteriole connections each time. We calculated the average likelihood that an occlusion would lead to loss of perfusion and likely ischemia (i.e. that an occlusion was upstream of an isolated arteriolar tree), and thus calculated the average percentage of tissue that lost local perfusion following an obstruction. We assumed that occlusions are equally likely to occur on each of the input arterioles.

RESULTS

Balb/c and C57Bl/6 mice have dendritic and arcaded arteriolar trees, respectively

Whole-muscle montaged images revealed striking differences between the skeletal muscle arteriolar trees of mice of different strains (Figure 1). The spinotrapezius arteriolar networks of C57Bl/6 mice exhibited a heavily ramified arcade structure, with multiple input arterioles feeding into a net of arteriolar channels (arteriole-to-arteriole linkages) and supplying short terminal arterioles (Figure 1A, arterioles in red). In contrast, the networks of Balb/c mice had a dendritic structure, in which each input arteriole feeds an independent tree of terminal

arterioles, with few arteriolar-level connections to the other inputs (Figure 1B, arteriole trees in red, green or blue). For each of these inbred strains, all mice tested had similar arteriolar structures (Figure 1C–E); each C57Bl/6 muscle was fed by only one or two arteriolar networks, while in Balb/c mice, the tissue volume was a patchwork of independent regions ('watersheds') each fed by a specific arteriolar tree with only one or two input arterioles per watershed. These morphologies were not specific to the spinotrapezius; they were also observed in the latissimus dorsi (Figure 1F–H) and thoracic diaphragm (Figure 1I,J). Coupled with previous observations [3], this suggests that Balb/c mice have dendritic, unconnected arteriolar trees in all or most tissues, a possible root cause for observed vulnerability to various ischemic diseases [1,3,6,9,10,14]. Interestingly, no clear differences were noted between the venular trees of mice of different strains in the muscles tested; spinotrapezius and latissimus dorsi venule-to-venule connections appeared to be common in both strains (Figures 1A, B, G, H). No significant gender differences in arteriolar architecture were noted in mice of either strain (Figures 1E, F).

Arteriolar ligation upstream of the spinotrapezius results in regional loss of perfusion in Balb/c but not C57Bl/6 mice

We noted previously that ligation of an upstream spinotrapezius arteriole in C57Bl/6 mice led to arteriolar diameter expansion, increased tortuosity and increased arteriolar length density as measured by smooth muscle alpha-actin coverage [2]. These are remodeling behaviors consistent with changes in the blood flow patterns downstream of the ligation, however it was not clear whether ischemia (including but not limited to complete and sustained loss of perfusion) took place. Following ligation of the spinotrapezius arteriole, we injected fluorescently-labeled lectin (*see Methods*) into the jugular vein, to indicate which tissue regions were experiencing a loss of blood flow. No ischemic areas were noted in C57Bl/6 mice as early as 5–10 minutes following ligation (Supplemental Figures S6A, S7). Despite the fact that perfusion was (at least partly) maintained, significant rearrangement of flow direction in many of the vessels downstream of the ligation would have been necessary to effectively re-route flow around the obstruction. This adjustment of flow pattern appears to lead to the increased tortuosity in ligated C57Bl/6 spinotrapezius arterioles [2].

However, in Balb/c mice, a region of complete perfusion loss and likely ischemia, as indicated by the absence of lectin staining, was clearly visible downstream of the ligated arteriole. The capillary networks of other arteriolar watersheds were perfused (Figure 2A, Supplemental Figures S6C, S9), but even though these capillaries were directly connected to the ischemic capillaries they did not aid in perfusion (Supplemental Figure 6D). The region of perfusion loss was almost exactly coincident with a hypothetical arteriolar 'watershed' based on Voronoi tessellation of the muscle following seeding of regions by outlining the arteriolar tree itself, suggesting no cross-perfusion by the adjacent arteriolar trees (Figure 2B). Perfusion loss was not observed in sham-ligated (data not shown) or contralateral muscles (Supplemental Figures S6B, S8).

Perfusion of the Balb/c spinotrapezius recovers over time

After one day, the likely ischemic regions downstream of ligated arterioles remained unperfused (Figure 3A,B). However, over the course of one week, perfusion returned to the region; first to the arteriole (day 2) and then to the capillaries. Although the volume of tissue distant from perfused vessels reduced significantly at day 2, it is arterioles and not capillaries that are reperfused first, consistent with perfused capillaries forming arteriole-to-arteriole collaterals, as opposed to directly feeding capillaries in the region downstream of the ligated arteriole. By day 7, not all capillaries appeared to be perfused, but there was no large portion of the region that did not demonstrate a restoration of blood flow (Figure 3C). As noted above for mice on day 0, most of the tissue outside the target watershed remained

perfused during this period (Figure 3D). The restoration of perfusion was accompanied by increased arteriole-to-arteriole connections, as evidenced both by fewer watersheds (Figure 3E) and a large increase in individual connections (Figure 3F), compared to either contralateral muscles or sham-ligated muscles of littermates. Comparable increases in arteriolar connectivity were observed in both male and female Balb/c mice.

Capillary arterIALIZATION connects isolated arteriolar trees following arteriolar ligation in Balb/c mice

The recovery in Balb/c perfusion was coincident with the emergence of vascular structures that surrounded the presumed ischemic region and connected the ischemic arteriolar tree to the adjacent trees, each of which were fed by various nonligated input arterioles (Figure 4A–D).

These new structures were parallel to the muscle fibers and to the capillary bed (Figure 4C–E). They were straight, non-tortuous and parallel to the prevailing capillary direction in all cases. As no increase in the vessel density is observed in this region (Figure 4G), these structures appear to be pre-existing capillaries that are undergoing diameter expansion and arterIALIZATION through the recruitment of new smooth muscle cells (Figure 4F; note correlation of diameter with actin expression). Although not all of the capillaries underwent expansion and arterIALIZATION (Figure 4F, 4H, Supplemental Figure S10), this is not required for a significant decrease in the resistance to flow between the arteriolar trees (Supplemental Figure S10, Figure 4I), assuming the capillaries act as parallel flow conduits. Capillary arterIALIZATION was not observed in sham-ligated or contralateral muscles. The location of the arterIALIZATION was demonstrated to be specific to the ligation location, as an alternate ligation site (an arteriole feeding an isolated region of muscle) produced capillary arterIALIZATION only in that region but not in the main tissue (Supplementary Figure S11).

Mice of the outbred strain CD1 exhibit either Balb-like or C57-like morphology and response

For an outbred mouse strain such as CD1, we expected more interindividual variability than for the inbred strains. However, while not all CD1 mice examined were identical, they typically fell into one of two categories: those with C57-like arteriole arcades and those with Balb-like dendritic arterioles (Figure 5A–C). Particularly notable is that mice appeared to be entirely one type or the other based on the muscle vasculatures that were tested. That is, spinotrapezius and latissimus dorsi, on both the left and right sides, had similar arteriolar morphology in each mouse (Figure 5D–E).

The C57-like and Balb-like CD1 mice responded to arteriolar ligation in the same manner as the inbred strains that they resemble; that is, increased arteriolar tortuosity for C57-like (Figure 5F) or capillary diameter expansion for Balb-like (Figure 5G). Although the Balb-like CD1s had a similar low frequency of arteriole-to-arteriole collaterals as Balb/c mice (Figure 5C), in the CD1s these collaterals were often located downstream of the arteriole targeted for surgical ligation, thus linking the ligated arteriolar tree to another perfused tree. In this case, the capillary diameter expansion was not seen following ligation, and instead diameter expansion and increased tortuosity of those arteriole-to-arteriole links occurred (Figure 5H). Indeed, in the rare case where an inbred Balb/c mouse was observed to have a pre-existing arteriole-to-arteriole collateral downstream of the ligated arteriole, we again observed arteriolar remodeling and tortuosity rather than capillary arterIALIZATION (Supplemental Figure S12). In addition, arteriolar ligation in A/J mice, which also exhibit Balb/c-like dendritic arteriolar structure (not shown) and increased vulnerability to ischemic injury [6], also showed capillary arterIALIZATION, though only small numbers of mice were tested (Supplemental Figure S13). Thus, it appears that the microvascular remodeling

response to decreased arteriolar flow can be predicted by the arteriolar network morphology, specifically the presence and location of arteriole-to-arteriole collaterals.

Long-term status of new arterioles

To determine whether the new arteriolar structures generated following the arteriolar ligation in Balb/c and other mice of similar morphology were temporary, spinotrapezius muscles were harvested two, three and six weeks following ischemic ligation in Balb/c and A/J mice. Interestingly, the connections between the ligated arteriole and those of nearby watersheds remained; however, they appeared to be fewer and of larger diameter, suggesting that a subset of the original arterializing capillaries may become long-lasting higher-caliber collateral vessels while the others regressed (Figure 6).

Theoretical analysis of ischemic occlusions in dendritic arteriolar networks

Using a model of multiple independent arteriolar trees feeding a tissue, we explored the impact of simulated ischemic arteriolar blockages in tissues with and without a small number of randomly-placed pre-existing arteriole-to-arteriole collaterals (Figure 7A–B). For each point on the graphs, we randomly generated 10,000 connected arteriolar networks, and calculated for each the likelihood that an arteriolar occlusion will occur on an isolated arteriolar tree causing a loss of perfusion and likely ischemia (Figure 7A), and the expected value of the percentage of tissue impacted by an occlusion (Figure 7B). It is interesting to note that even a small number of arteriole-to-arteriole connections significantly reduced the risk of poor outcome following occlusions or ligations; for example, three connections reduced the expected tissue loss to 6%; ten connections reduced it almost to zero (Figure 7B). While this analysis abstracts details such as the relative diameters of the collaterals and the occluded vessels, this is a useful first estimate of the degree of connectedness that is required to confer ischemia-protectedness. In addition, this method can be a useful tool for judging the vulnerability or protectedness of actual mouse or patient microvascular networks.

DISCUSSION

In this study, we have shown that the pre-existing arteriolar network morphology – the microvascular phenotype – of the spinotrapezius muscle indicates both the severity and duration of perfusion loss (and possible ischemia) following an occlusion and the type of microvascular remodeling response to that occlusion over time. For arcaded arterioles, such as in C57Bl/6 and some CD1 mice, although there is likely to be a significant rearrangement of flow direction in some vessels downstream of the ligation, no discernable loss of perfusion is observed (as early as 5–10 minutes following ligation, perfusion appears to be present throughout the muscle), and the blood flow changes lead to morphological changes in some of the pre-existing arteriole-to-arteriole collaterals – specifically, increased tortuosity (Figure 5F, schematic Figure 7C). This matches previous observations in the mouse spinotrapezius[2] and in the rabbit hindlimb[7]. In contrast, for dendritic networks with fewer collaterals at the arteriolar level, such as in Balb/c and some CD1 mice, perfusion loss clearly follows vascular occlusion (Figure 2). Without low-resistance arteriolar collateral pathways, capillaries remodel over time, not by becoming tortuous but by increasing diameter and becoming arterialized to carry the load of re-routing blood (Figure 4; schematic Figure 7C).

The arterialization – that is, the expression of arterial markers along an enlarged capillary – requires either smooth muscle cells to be recruited (e.g. by migrating or proliferating downstream from existing arterioles), or preexisting cells (e.g. pericytes) to newly express smooth muscle markers and act as arteriolar support cells. It is not clear, from our

observations, which process is taking place, but the co-location of the novel smooth muscle α -actin with the diameter-expanded capillaries suggests that the smooth-muscle marker-expressing cells are required for vessel stability and enlargement.

That these arterIALIZED capillaries are collaterals from one arteriole tree to another was confirmed by visual inspection. First, they do not connect arterioles with venules; second, they do not terminate in mid-capillary, but run from terminal arteriole to terminal arteriole. In addition, the morphology of these newly arterIALIZED vessels makes it clear that these are former capillaries rather than extended arterioles; while terminal arterioles are somewhat tortuous and not oriented, both capillaries and the 'new' vessels are straight, less tortuous and parallel to the muscle fibers.

The expansion of only a subset of the capillaries (Figure 4G,H) suggests a 'rich-get-richer' feedback model for growth: there is initial variability in the diameter of capillaries (Supplemental figure S10), and the capillaries that are slightly larger form a lower-resistance pathway to flow. If increased flow causes growth, resistance is further lowered, increasing flow and so on. Testing this feedback loop requires longitudinal study of capillary remodeling in single mice, which is beyond our scope here.

The differing microvascular morphologies observed – from the extremes of C57Bl/6 and Balb/c, to the more varied CD1 mice – suggest a strong correlation between interindividual variability of microvascular architecture and susceptibility to damage following ischemic events (as noted in the introduction, Balb/c mice have more severe injuries following occlusions in both muscle and brain [1,3,6,9,10,14]). The twin mouse models of *ischemia-protected* and *ischemia-vulnerable* vasculature allows us to explore individual variability in the mouse, and provide a platform for testing therapies that decrease the vulnerability of tissue.

What makes this study unique is the level of the microvasculature that is being imaged in the skeletal muscle following arteriolar ligation: we are looking both at smaller vessels than previously investigated, and at whole-muscle networks of arterioles, venules and capillaries. This allows us a new window into the structural microvascular remodeling that takes place following vascular occlusions that has not been imaged in thicker tissues, such as the gracilis or other hindlimb muscles, or cardiac muscle. By using a perfused immunofluorescent marker, we also demonstrate for the first time sharp borders on the extent of perfusion loss (and likely, ischemia) following occlusion. This well-defined injury site would likely not be visible using other perfusion-measuring techniques such as Laser Doppler imaging, which are dominated by the flows of larger vessels.

Also novel in this study is our identification of two previously unidentified subgroups within the outbred CD1 strain. These groups demonstrate either C57Bl/6-like or Balb/c-like arteriolar structures in the spinotrapezius and latissimus dorsi, but most surprisingly, the visualized muscles of each mouse (whether by intravital or immunofluorescent imaging or both) were all of the same type, suggesting an underlying genetic basis for the morphology that is nonetheless not fully penetrant. Siblings do not all have the same morphology (not shown). While this individual variability has not been previously noted, our observations of CD1 mice fit well with results from other groups; Faber et al noted that CD1 mice have a density of adductor collaterals similar to Balb/c, pial collateral density intermediate between Balb/c and C57Bl/6, and a plantar perfusion response following ischemia that is closer to that of C57Bl/6 after 7 days, but closer to that of Balb/c after 21 days [3–5]. This intermediate level of response is consistent with the presence in the outbred CD1 data of two subgroups each responding similarly to one of the two more extreme inbred lines.

We suggest for the first time that while it is common in personalized medicine to focus on the separation of subgroups by genetic or proteomic means, measurements of microvascular network architecture from tissue biopsies may in fact be sufficient to distinguish arteriophenotype, and may even be superior in a situation where the ischemic response is determined primarily by the preexisting vascular network structure, which may itself be a result of an extremely complex gene-protein network. The architecture is a measurable, gross tissue-level feature that could easily be measured clinically.

It is also important to note that the extent of the region of perfusion injury in the Balb/c mice was not related to microvascular density or other common metrics used to quantify blood vessels; instead, it was a result of network properties, the combination of connectivity and relative diameters of the connections. This suggests that simply growing new vessels (e.g. angiogenesis) may not be useful in treating or pre-treating these ischemic diseases; the addition of more low-caliber conduits would not help the recovery of perfusion (Figure 4 and Figure S10), and appropriately-sized collateral arterial vessels are required. This is consistent with a shift in thinking in the field of therapeutic revascularization, in which arteriogenesis (increase in size of arterioles) is now being suggested as a superior alternative to angiogenesis [12].

We believe that the ligated spinotrapezius model is of large potential utility in further studying ischemia and vascular remodeling. Though it shares many aspects of the standard hindlimb ischemia model, there are notable differences. First, we do not observe appreciable tissue damage following ligation of the spinotrapezius artery, even in the Balb/c mice, where necrosis and even autoamputation of the hindlimb can occur within one to two weeks. Instead, the recovery of perfusion in the spinotrapezius is faster (days instead of weeks [3,6]). We also speculate that the thickness of the tissue allows some oxygen diffusion from neighboring tissue to prevent complete anoxia within the unperfused region of the tissue, staving off necrosis. Second, the volume of tissue affected by the perfusion injury is smaller in the spinotrapezius for two reasons: it is a thinner tissue; and the artery ligated is of a lower caliber and a higher order (i.e. further down the vascular tree). This also means that the response we observe is more microvascular than macrovascular. This model is therefore a useful analog, because (a) microvascular responses are also taking place, at least at the periphery of the large-volume ischemic regions, and (b) the responses are likely to scale well; that is, smaller spinotrapezius arterioles have blood re-routed through capillaries, while the larger hindlimb arteries re-route through arterioles. The ratio of occluded vessel diameter to collateral conduit diameter is similar.

Studies by other groups have investigated the possible molecular basis for the microvascular differences between C57Bl/6 and Balb/c mice. Faber and colleagues have shown that high and low levels of VEGF expression in genetically modified mice result in increased and decreased response to hindlimb ischemia in CD1 mice [5]. They also showed that the response of VEGFA expression to hindlimb ischemia is significantly lower in Balb/c mice [3]. Interestingly, however, they observed no significant impairment in collateral density or perfusion recovery in mice that possess only one allele of the major endothelial receptor for VEGF, VEGFR2, and mice heterozygous for VEGFR1, showed only slightly reduced perfusion recovery 3 days post-ligation, along with a reduction in peri-collateral inflammatory cells [5]. Recently, they have shown that mice without both copies of the gene *cltc4* (encoding Chloride Intracellular Channel-4) exhibit greatly reduced collateral density, suggesting involvement in early vascular network formation [4]. Using DNA from F2 crosses (i.e., (C57Bl/6 × Balb/c) × Balb/c), Annex and colleagues identified a quantitative trait locus (QTL) linked to greater tissue necrosis and reduced perfusion recovery following ligation [6]. They further showed that C57Bl/6 substituted with chromosome 7 (where the QTL was found) from ischemia-vulnerable A/J mice showed slower recovery of perfusion

[6]. Expression QTL (of hippocampal mRNA) by Faber et al identified a candidate region in chromosome 17, in the vicinity of VEGF [3]. Our own observations in young pups suggest that the arteriolar looping structures characteristic of C57Bl/6 mice are already present shortly after birth (data not shown). However, along with discussion of how these different microvascular structures are formed must come the question of, why? Is there a difference between looped and interlocking-tree networks? Is there an evolutionary advantage to having either a looped, interconnected arteriolar structure or a dendritic, regional one? Certainly, ischemic diseases such as stroke, coronary artery disease and peripheral artery disease are strongly correlated with age and in humans primarily affect those beyond childbearing age, suggesting that there may not be evolutionary pressure to have looped (protected) structures. The structures may have a differential ability to adapt to extreme exercise, resulting in a fitness difference (i.e. a trade-off between adaptability/robustness and design/peak performance), but this is an open question. The fact that dendritic and looped networks are present in different mice of a more genetically diverse strain of outbred mice (CD1) may suggest that neither results in a loss of fitness, though a slight numerical advantage for mice with at least a minimum number of arteriole-to-arteriole collaterals is observed. However it would be speculation to draw substantial conclusions on fitness from this data.

Whether or not a fitness advantage exists, there is still a compelling human health reason to prefer interconnected arteriolar networks as a paradigm for extended life and improved quality of life following ischemic events. In seeking to render vulnerable tissues more 'C57-like', we may ask: how many arteriole-to-arteriole connections would be required to make the network less vulnerable? Certainly there is stochasticity involved, but our observations suggest that the arteriolar looping of C57Bl/6 mice might be unnecessarily frequent; even a few well-placed connections can result in a less severe injury, whether in CD1 (Figure 5H), Balb/c (Supplemental Figure S12) or a hypothetical tissue fed by several arterioles (Figure 7A–B).

As advances in Systems Biology move us towards an era of personalized medicine, it is now plausible to identify subgroups of people for whom different therapies may be identified as more or most effective. Here, we suggest that there are subgroups that might be classified according to their ability to recover from, or be protected against, ischemic injury, and moreover, that this classification can be assigned by looking at the patterns of microvascular connectivity in their arteriolar beds.

While it may be possible to determine an individual's vulnerability, preemptive ligation surgery may not be wise. Instead, a non-surgical method for the stable induction of previously absent arteriole-to-arteriole connections could be very effective, not at preventing ischemic occlusions, but for minimizing their impact. The mouse spinotrapezius is an excellent model for determining the molecular characteristics of the microvascular response, and for testing possible methods of encouraging greater network connectivity.

Supplementary Material

Refer to Web version on PubMed Central for supplementary material.

Acknowledgments

The authors thank Alexander M. Bailey and Thomas C. Skalak for advice and constructive criticism during this study.

SOURCES OF FUNDING

Support provided by: NIH-HL082838-02 (S.M.P.), NIH-T32-HL007284 (F.M.G; PI: B.R. Duling) and NIH-K99-HL093219 (F.M.G.).

REFERENCES

1. Aronowski J, Labiche LA. Perspectives on reperfusion-induced damage in rodent models of experimental focal ischemia and role of gamma-protein kinase C. *Ilar J* 2003;44:105–109. [PubMed: 12652005]
2. Bailey AM, O'Neill TJ, Morris CE, Peirce SM. Arteriolar remodeling following ischemic injury extends from capillary to large arteriole in the microcirculation. *Microcirculation* 2008;15:389–404. [PubMed: 18574742]
3. Chalothorn D, Clayton JA, Zhang H, Pomp D, Faber JE. Collateral density, remodeling, and VEGF-A expression differ widely between mouse strains. *Physiol Genomics* 2007;30:179–191. [PubMed: 17426116]
4. Chalothorn D, Zhang H, Smith JE, Edwards JC, Faber JE. Chloride intracellular channel-4 is a determinant of native collateral formation in skeletal muscle and brain. *Circ Res* 2009;105:89–98. [PubMed: 19478202]
5. Clayton JA, Chalothorn D, Faber JE. Vascular endothelial growth factor-A specifies formation of native collaterals and regulates collateral growth in ischemia. *Circ Res* 2008;103:1027–1036. [PubMed: 18802023]
6. Dokun AO, Keum S, Hazarika S, Li Y, Lamonte GM, Wheeler F, Marchuk DA, Annex BH. A quantitative trait locus (LSq-1) on mouse chromosome 7 is linked to the absence of tissue loss after surgical hindlimb ischemia. *Circulation* 2008;117:1207–1215. [PubMed: 18285563]
7. Eitenmuller I, Volger O, Kluge A, Troidl K, Barancik M, Cai WJ, Heil M, Pipp F, Fischer S, Horrevoets AJ, Schmitz-Rixen T, Schaper W. The range of adaptation by collateral vessels after femoral artery occlusion. *Circ Res* 2006;99:656–662. [PubMed: 16931799]
8. Hausler M, Sellhaus B, Scheithauer S, Gaida B, Kuroпка S, Siepmann K, Panek A, Berg W, Teubner A, Ritter K, Kleines M. Myocarditis in newborn wild-type BALB/c mice infected with the murine gamma herpesvirus MHV-68. *Cardiovasc Res* 2007;76:323–330. [PubMed: 17658501]
9. Helisch A, Wagner S, Khan N, Drinane M, Wolfram S, Heil M, Ziegelhoeffer T, Brandt U, Pearlman JD, Swartz HM, Schaper W. Impact of mouse strain differences in innate hindlimb collateral vasculature. *Arterioscler Thromb Vasc Biol* 2006;26:520–526. [PubMed: 16397137]
10. Majid A, He YY, Gidday JM, Kaplan SS, Gonzales ER, Park TS, Fenstermacher JD, Wei L, Choi DW, Hsu CY. Differences in vulnerability to permanent focal cerebral ischemia among 3 common mouse strains. *Stroke* 2000;31:2707–2714. [PubMed: 11062298]
11. Rasband, WS. Bethesda, Maryland, USA: U. S. National Institutes of Health; 1997–2009. ImageJ. <http://rsb.info.nih.gov/ij/>
12. Schaper W. Collateral circulation: past and present. *Basic Res Cardiol* 2009;104:5–21. [PubMed: 19101749]
13. Schierling W, Troidl K, Troidl C, Schmitz-Rixen T, Schaper W, Eitenmuller IK. The role of angiogenic growth factors in arteriogenesis. *J Vasc Res* 2009;46:365–374. [PubMed: 19142016]
14. Sugimori H, Yao H, Ooboshi H, Ibayashi S, Iida M. Krypton laser-induced photothrombotic distal middle cerebral artery occlusion without craniectomy in mice. *Brain Res Brain Res Protoc* 2004;13:189–196. [PubMed: 15296857]

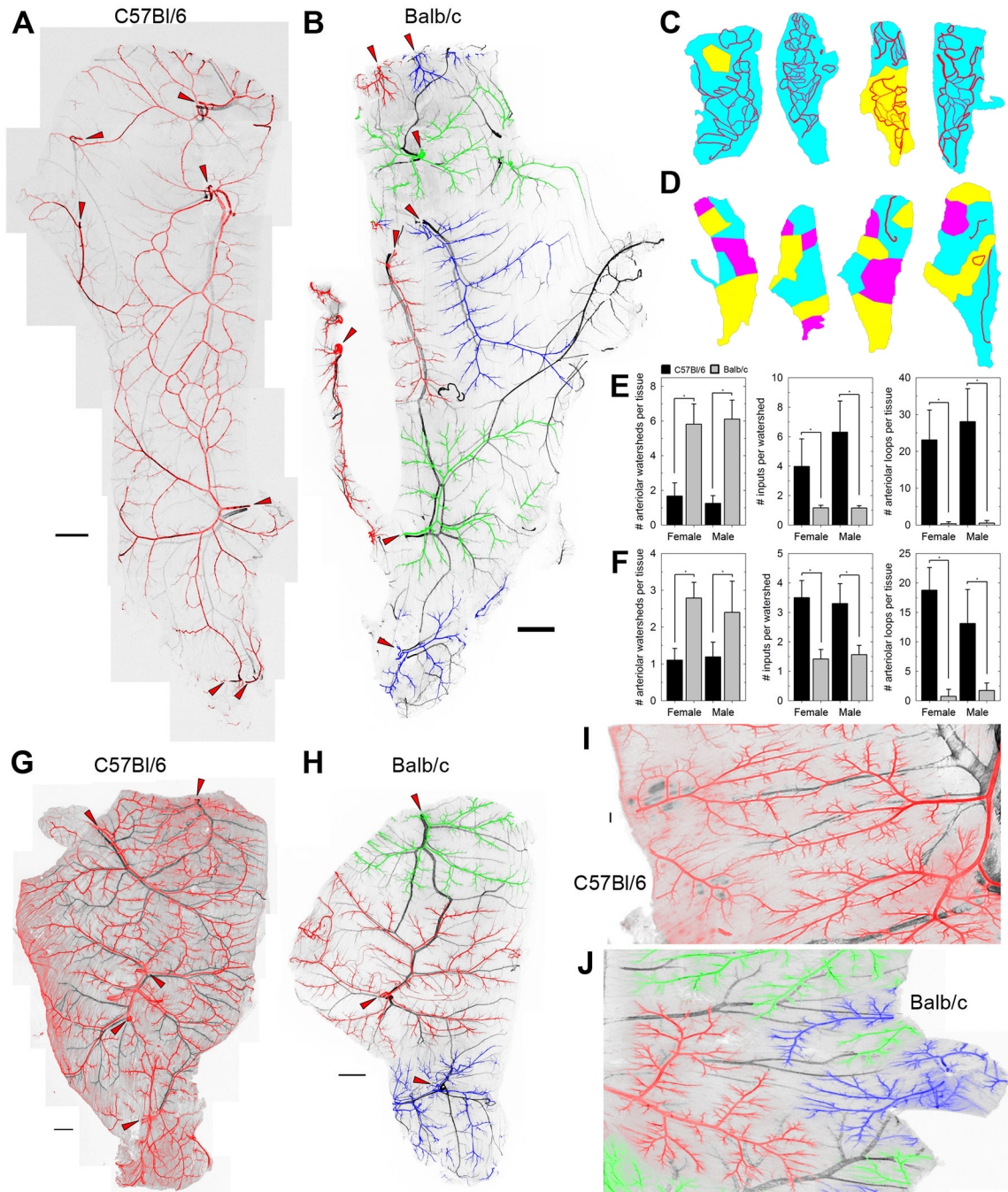


Figure 1. Arteriolar and venular networks in mouse skeletal muscle

A and B, Typical spinotrapezius muscles of C57Bl/6 and Balb/c mice, immunofluorescently stained for smooth muscle α -actin. Veins are shown in black; arterioles are pseudocolored red, green or blue, with adjacent connected arteriolar trees having the same color.

Nonadjacent arteriolar trees of the same pseudocolor are not connected at the arteriolar level within the tissue; that is, each of the green, blue and red arteriolar trees are distinct from one another. The arteriolar inputs into the muscle are indicated by red arrowheads. Higher-resolution versions are given in Supplemental Figures S2 and S3. **C and D,** Variability in the watersheds and arteriole-to-arteriole collaterals of C57Bl/6 (C) and Balb/c (D) spinotrapezius muscles. Watersheds are defined as volumes of tissue that are fed by a single

arteriolar network, pseudocolored as the networks are in A. Arteriolar-level connections between the arteriolar trees downstream of the multiple arteriolar inputs into the tissue are shown in red. **E and F**, Quantification of the morphological differences in spinotrapezius (E) and latissimus dorsi (F) arteriolar structure of the mouse strains. The metrics that best differentiate the strains are the number of arteriolar inputs that supply each watershed (a measure of the interconnectedness of the arteriolar trees) and the presence of arteriolar loop structures within the tissue. $n=4-18$ per group; *, $P<0.001$ by ANOVA. **G and H**, Typical latissimus dorsi muscle of C57Bl/6 and Balb/c mice, stained and pseudocolored as in A and B. The arteriolar inputs into the muscle are indicated by red arrowheads. High-resolution versions are given in Supplemental Figures S4 and S5. **I and J**, Comparable regions of typical thoracic diaphragm muscles of C57Bl/6 and Balb/c mice, stained and pseudocolored as in A and B. Scale bars for A, B, G, H, 1 mm; scale bar for I, J, 200 μm .

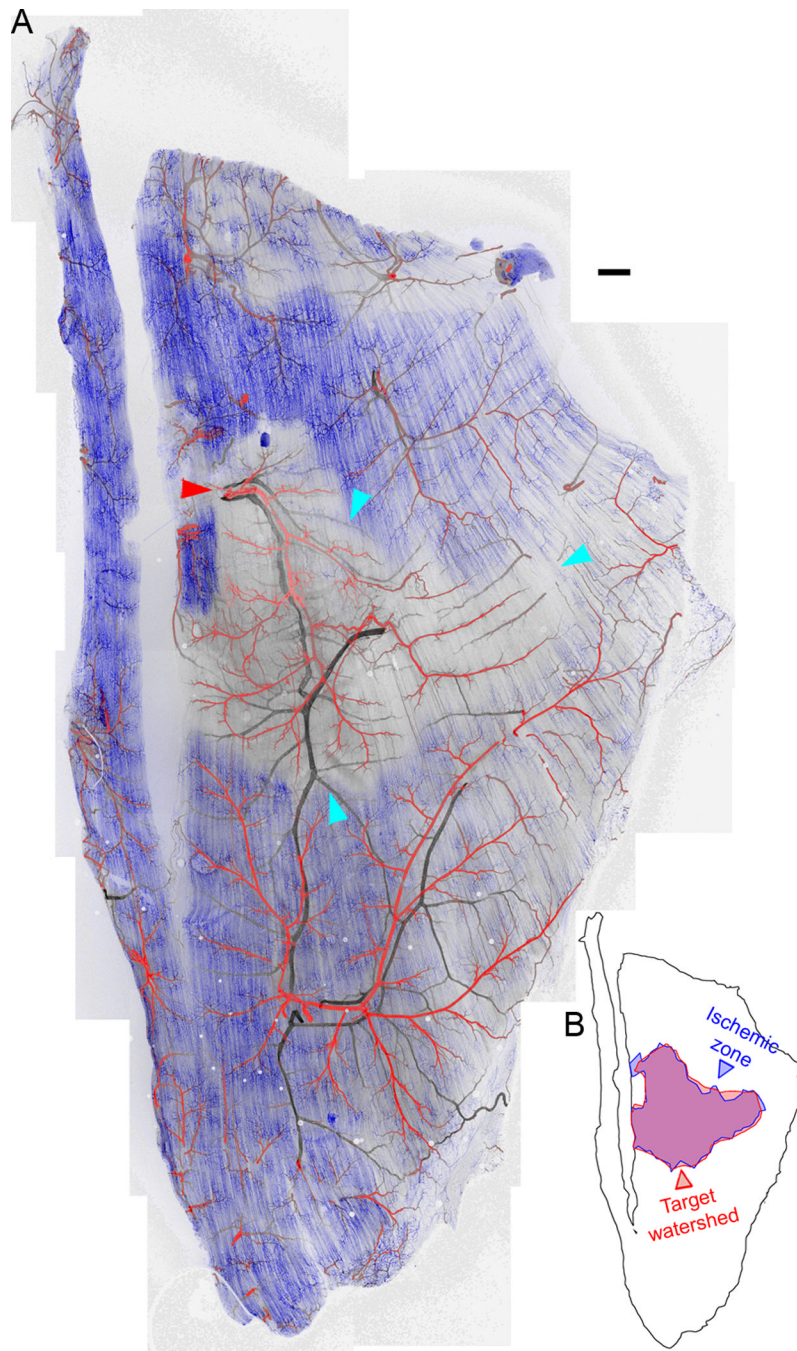


Figure 2. Loss of perfusion immediately following arteriolar ligation in Balb/c mice
A, Perfusion of capillaries (blue, fluorescent intravenous lectin) was lost in part of the Balb/c spinotrapezius immediately post-ligation. The ligation site is indicated with a red arrowhead. The perfusion-poor volume is outlined with cyan arrowheads. This loss of perfusion was not observed in the contralateral muscle, or in ligated muscles of C57Bl/6 mice (Supplemental Figure S6). Red, arteries; black, veins. **B**, The perfusion-poor region is almost exactly contiguous with the watershed of the ligated arteriole. Scale bar for A, 250 μm .

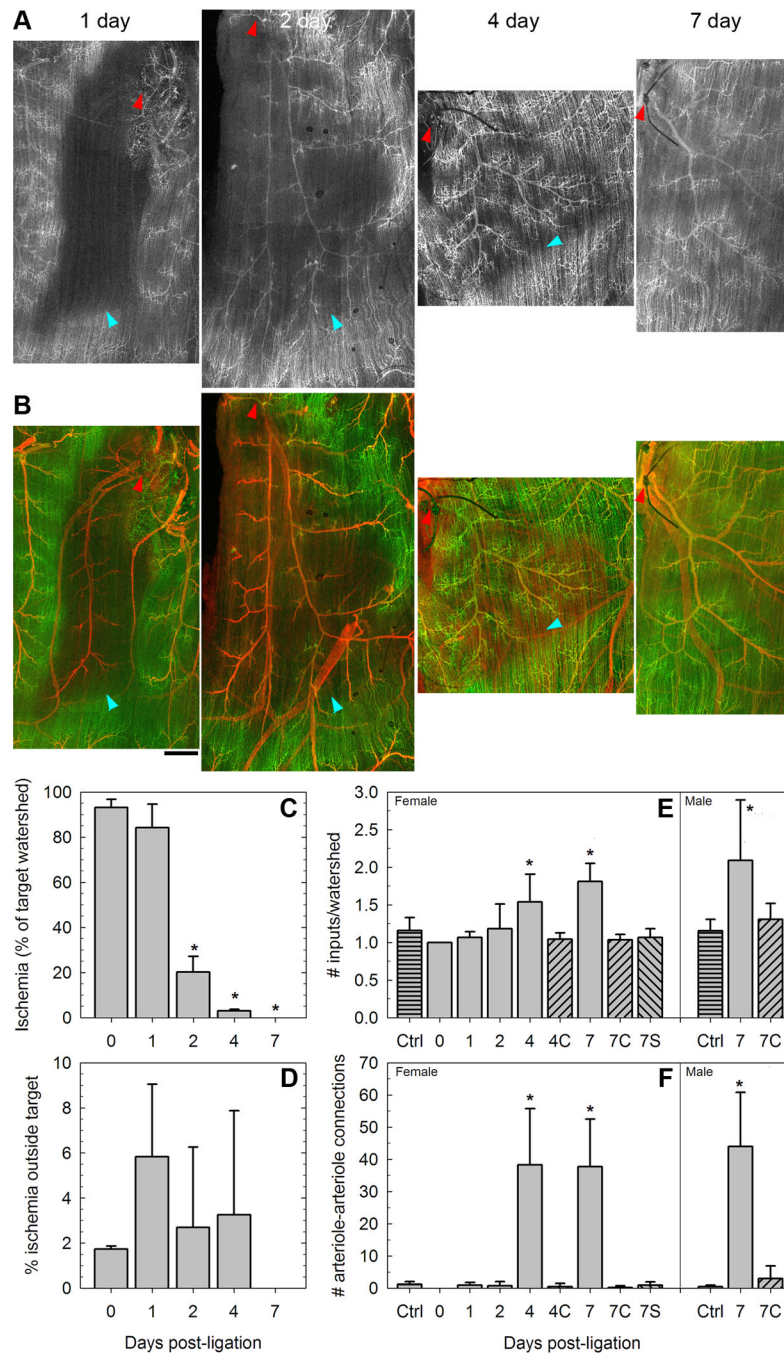


Figure 3. Reperfusion of Balb/c muscles following arteriolar ligation

A and B, Perfusion of arterioles and capillaries of Balb/c muscles 1–7 days following ligation of the spinotrapezius artery. The ligation site is indicated by a red arrowhead. Perfusion-poor regions between still-perfused and newly-reperfused tissue are indicated by cyan arrowheads. Scale bar, 100 μ m. **C**, The volume of the target watershed (i.e. of the tissue fed by the arteriole downstream of the ligation) experiencing zero perfusion in the days following ligation. N=3–4 per group. *, P<0.01 as determined by one-way ANOVA. **D**, Little of the perfusion loss is outside of the target watershed volume. N=3–4 per group. **E and F**, The perfusion recovery is accompanied by an increase in the arteriole-to-arteriole connectivity of the tissue, enlarging the watersheds (E) and increasing collateral arteriolar

pathways (F). $N \geq 4$ per group (females), $N \geq 5$ per group (males). *, $P < 0.01$ as determined by two-way ANOVA and Tukey's test. Days 4 and 7 were significant with respect to controls ("Ctrl"), contralateral (non-ligated) muscles ("C"), and sham-ligated mice ("S").

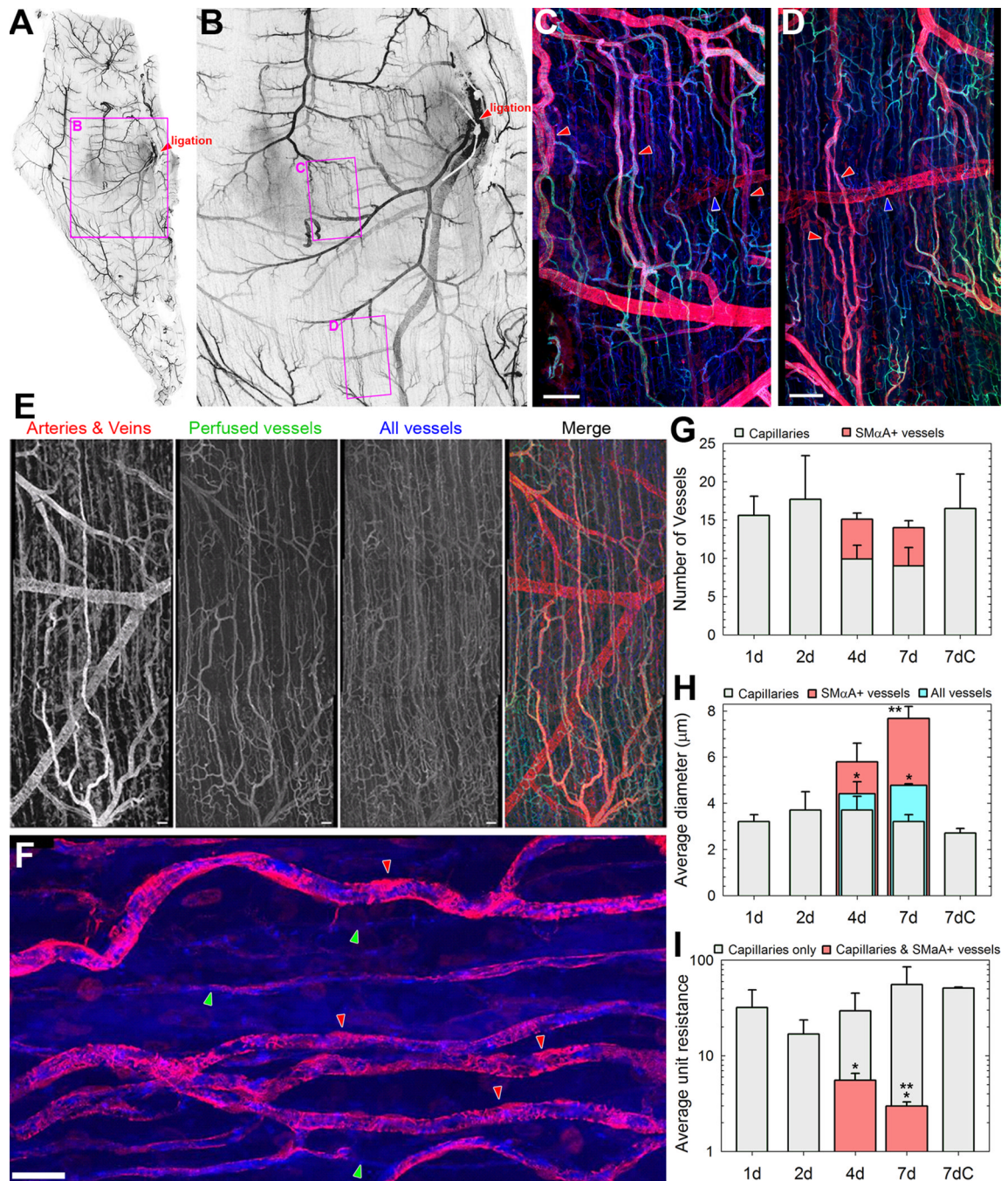


Figure 4. Collateral capillary arterialization in Balb/c mouse spinotrapezius

A and B, Balb/c spinotrapezius muscles show the presence of arterialized capillaries that are connecting the targeted (ligated) arteriolar tree to a neighboring, perfused network, seven days after ligation. Montage of smooth muscle α -actin images. Ligation site indicated by red arrowhead. **C and D**, Close-up of the arteriolar structures in B. Red, smooth muscle α -actin; green, perfused lectin; blue, superperfused lectin. Red arrowheads, arterialized capillaries; blue arrowheads, veins. Scale bars, 100 μ m. **E**, Perfusion of arterialized capillaries, showing the expansion of capillary diameter that accompanies the arterialization. Red, smooth muscle α -actin; green, perfused lectin; blue, superperfused lectin. Scale bars, 50 μ m. **F**, Close-up (600 \times) of arterialized capillaries, highlighting the relationship between vessel diameter and smooth

muscle α -actin coverage. Red arrowheads, enlarged capillaries; green arrowheads, regular-diameter capillaries. Red, smooth muscle α -actin; blue, superfused lectin. Scale bar, 50 μ m. **G–I**, Quantification of the arteriole-to-arteriole connections in ligated and nonligated skeletal muscle. There is no significant variation in total vessel density (G) or the average diameter of actin-negative capillaries (H) or the average unit resistance of actin-negative vessels (I). 1d, 1 day post-ligation. 7dC, contralateral muscle 7 days post-ligation. *, significant change in average diameter of all vessels or average unit resistance of all vessels $p < 0.05$ by one-way ANOVA. **, significant increase from 4 days to 7 days $p < 0.05$ by t-test. N=3 mice per group; 3 ipsilateral and 3 contralateral regions per mouse.

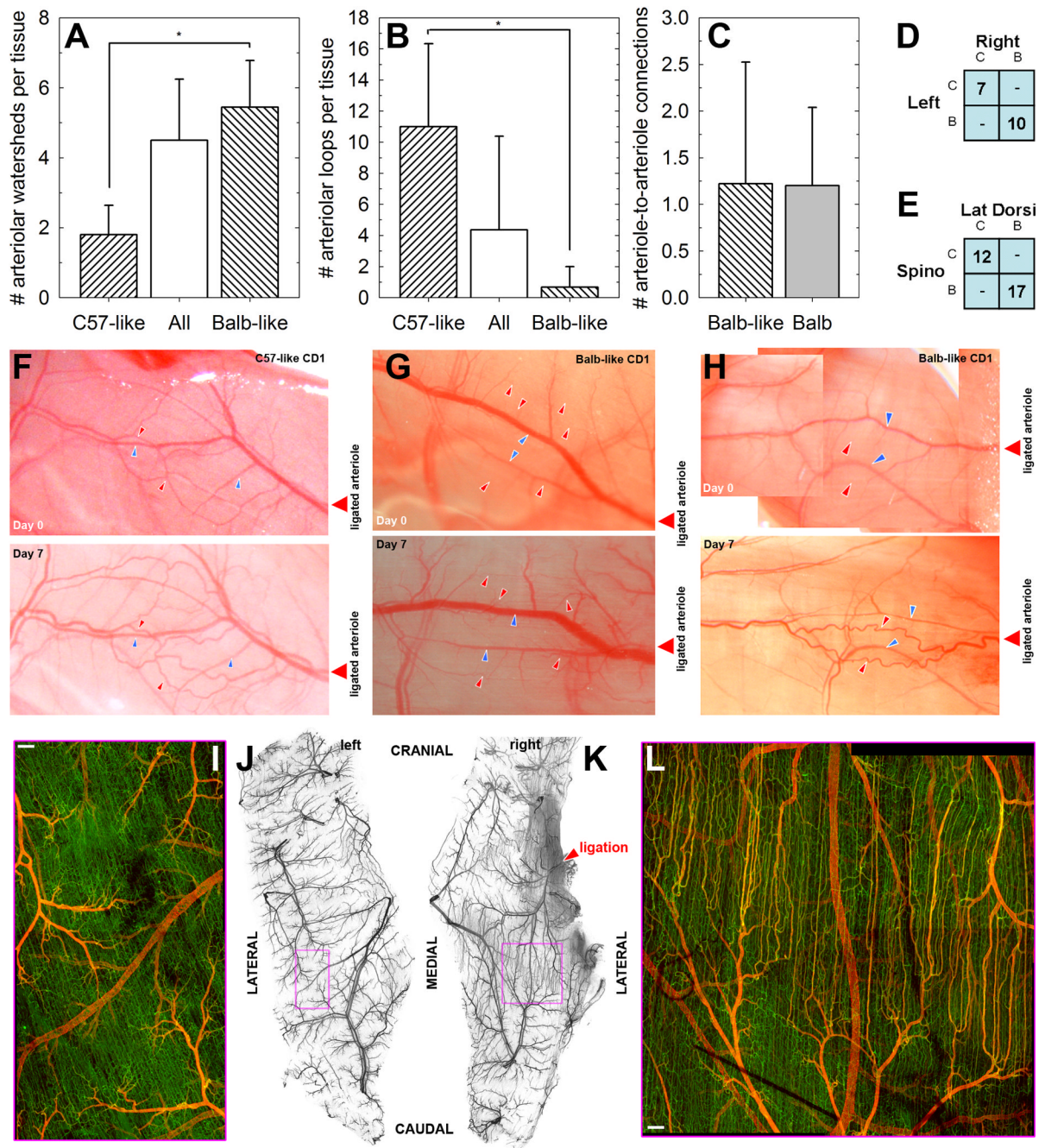


Figure 5. Microvasculature of CD-1 mice, an outbred strain, resembles either C57Bl/6 or Balb/c and responds as predicted

A–C, CD-1 mice exhibit either C57-like (highly-connected) arteriolar morphology or Balb-like dendritic morphology. *, $P < 0.01$ by t-test comparison between C57-like and Balb-like subgroups. $N = 5$ (C57-like), $N = 9$ (Balb-like). **D**, The left and right spinotrapezius muscles of each mouse are consistently C57-like ('C') or Balb-like ('B'). **E**, The spinotrapezius and latissimus dorsi muscles of each mouse are consistently C57-like ('C') or Balb-like ('B'). **F–H**, Intravital images of CD-1 mice. Both C57-like and Balb-like morphologies are seen in CD-1 mice. On day seven following arteriolar ligation, C57-like networks demonstrate remodeling at the arteriolar level (increased tortuosity and diameter, panel F), as seen for

C57Bl/6 mice [2]. Balb-like networks do not demonstrate remodeling of existing arterioles but rather diameter expansion in the capillaries (panel G). Where a Balb-like dendritic arteriolar network includes an arteriole-to-arteriole connection downstream of the ligation, remodeling is more similar to C57Bl/6 mice (panel H). Red arrowheads, arterioles; blue arrowheads, venules. **I–K**, The capillary arterialization observed in Balb/c mice following arteriolar ligation is recapitulated in Balb-like CD1 mice. I and L show comparable inter-arterial regions in ligated (L) and contralateral (I) muscles, magnified from boxed regions in J and K respectively; while there are connections between the capillaries at the capillary level, the contralateral side exhibits no arterialization.

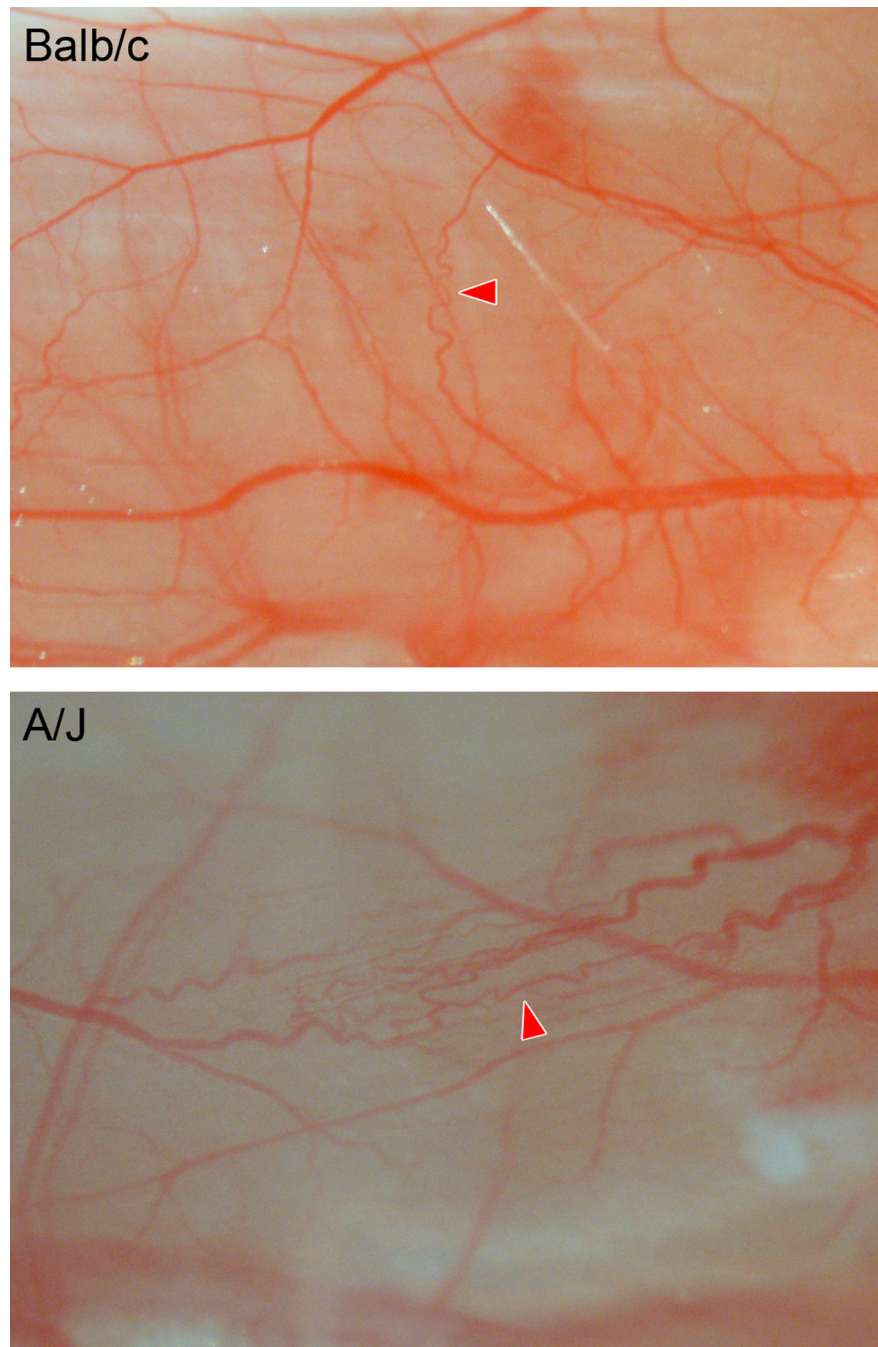


Figure 6. Long-term stability of arterIALIZED capillaries
Spinotrapezius muscles imaged 40 days (Balb/c) or 42 days (A/J) after arterial ligation. Arteriole-to-arteriole connections (red arrowheads) persist at this timepoint, suggesting their long-term stability.

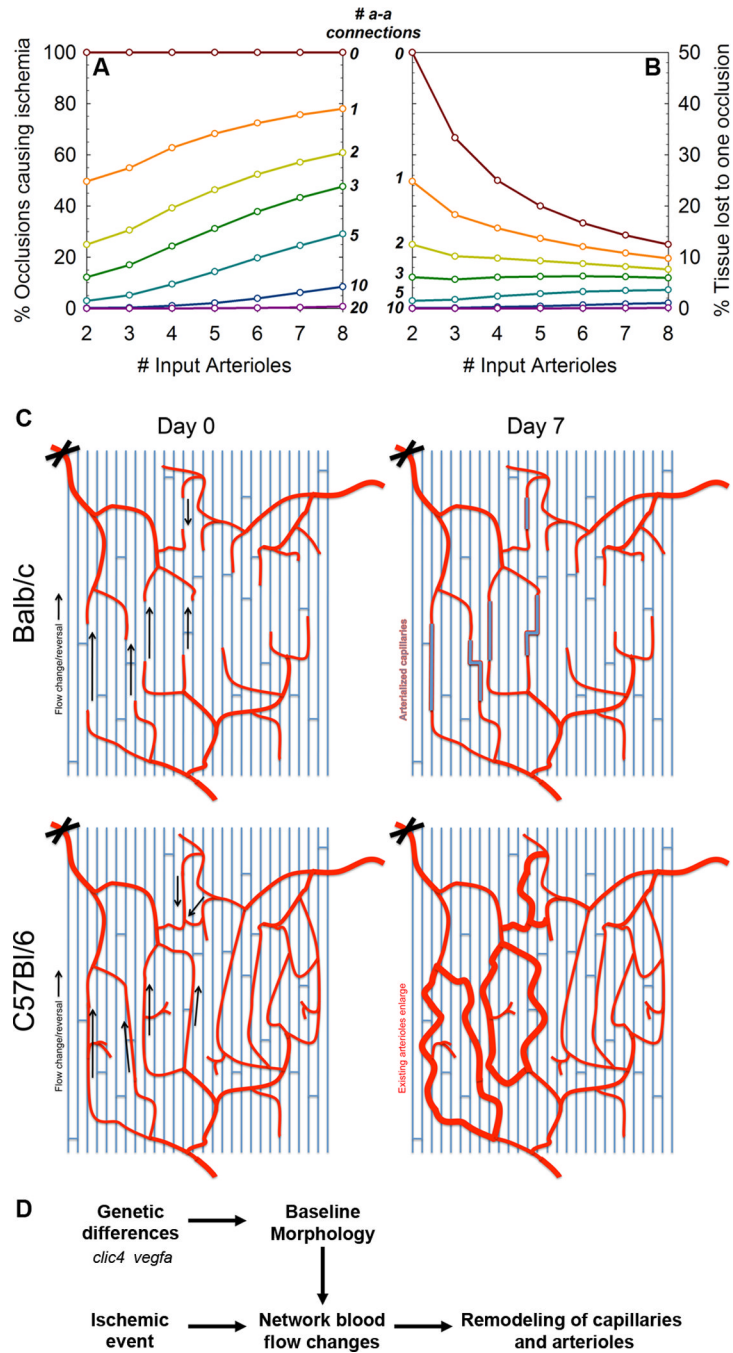


Figure 7. Vulnerability of Balb-like networks

A, Percentage of arterial occlusions that are predicted to cause loss of perfusion and ischemia in a tissue, assuming 0–3 similar-diameter arteriole-to-arteriole collaterals are present. **B**, Predicted average percentage of tissue downstream of an occlusion. **C**, Schematic of the blood flow changes (left, arrows) and morphological changes (right) following arteriolar ligation of Balb/c (top) and C57Bl/6 (bottom) mice. **D**, Schematic of the development of muscle vasculature and subsequent responses to loss of perfusion and flow re-routing. Genes such as *cltc4* and *vegfa* have been shown to be involved in the formation of arteriole-to-arteriole collaterals.